Electronic conductance in mesoscopic systems: multichannel quantum scattering calculations

1995 J. Phys.: Condens. Matter 7 6045

(http://iopscience.iop.org/0953-8984/7/30/009)

J. Phys.: Condens. Matter 7 (1995) 6045–6063. Printed in the UK

Electronic conductance in mesoscopic systems: multichannel quantum scattering calculations

I Tuvi†, Y Avishai‡ and Y B Band†‡

† Department of Chemistry, Ben-Gurion University, Beer-Sheva, Israel

‡ Department of Physics, Ben-Gurion University, Beer-Sheva, Israel

Received 18 November 1994, in final form 26 January 1995

Abstract. Multichannel quantum scattering theory is employed to calculate the non-linear two-port conductance and magnetoconductance of mesoscopic systems such as quantum well heterostructures, quantum dots and semiconductor or metallic microstructures. We employ a specially designed stable invariant embedding technique for calculating reflection and transmission amplitudes for these types of structure using a quantum rearrangement scattering formulation. The method can be applied to calculate electronic transport in many types of system in the low-temperature regime where phonon scattering is not significant. The basis set used for the degrees of freedom orthogonal to the current flow can be adiabatic (i.e. dependent on the coordinate along the current flow) or diabatic (not dependent on the coordinate). The dangers inherent in transforming an adiabatic formulation to a diabatic formulation with a limited basis set size are forcefully illustrated. The method naturally includes closed-channel effects and can incorporate complex potentials (to simulate decay). Examples are presented, wherein we calculate the conductance and magnetoconductance as a function of system geometry, electronic potential and potential drop across two-dimensional quantum well heterostructures, and the results are explained in simple physical terms. The resonance features in the non-linear conductance as functions of magnetic field and of orifice width in heterostructure devices are described and elucidated.

1. Introduction

Interest in electrical conductance in mesoscopic systems has been enhanced by significant technological advances in the fabrication of heterostructures and superlattices as well as startling discoveries such as the observation of a Coulomb blockade in quantum tunnelling, ballistic electronic conduction, current that is non-linear in the applied voltage drop across a device (e.g. negative differential resistance characteristics of semiconductor heterostructures) [1–4], and improved understanding of the effects of electron localization and disorder on conductance [4–7]. These phenomena are enabling a revolution to occur in electronics.

In this paper we employ a multichannel quantum scattering method for calculating the conductance of heterostructure interfaces, based upon an invariant embedding technique [8–12] to determine the non-linear conductance of quantum well devices. We explicitly consider the case when the channels to the right and left of the interface are different from each other because of the potential drop across the interface [12]. Calculations of the conductance of heterostructure devices (e.g. resonant tunnelling barrier structures) have been most often carried out using a (zero-order) Hamiltonian with the same asymptotic limits of the potential to the left and right of the device [13]. When the potential drop across the device is sufficient to produce a non-linear conductance, calculation of the conductance must explicitly take into account the difference between the asymptotic potentials to the left

0953-8984/95/306045+19$19.50

and right of the device. Our specially designed invariant embedding method [12] which we use for calculating the reflection and transmission amplitudes is capable of accurate and extremely stable propagation across large classically forbidden (and classically open) regions. An explanation of the stability of invariant embedding method is contained in [8] and a description of how to include closed channels in these calculations is contained in [11]. Standard methods that propagate the Schrödinger wavefunction suffer from instabilities in treating such problems, and logarithmic derivative methods cannot be used because of the nature of the boundary conditions of the kind of problem treated here. Moreover, the method can also easily include the details of the geometry of the system within the calculation because the method is capable of treating the scattering in an adiabatic basis set formulation [11, 12]. Using our method we can consider one-, two- or three-dimensional models of quantum well heterostructures, quantum dots, and semiconductor or metallic microstructures. The two- or three-dimensional calculations are multichannel generalizations of the one-dimensional calculation (which itself is a two-channel problem) necessary to treat the transverse coordinates of the quantum well within a basis set representation. We shall not consider procedures for self-consistently determining the potential and the transport properties, nor shall we consider inelastic scattering events (although we should mention that a decay rate for each channel can be easily incorporated in order to simulate decay of the electronic wavefunction due to phonon scattering, but this is inadequate unless the phonon scattering is very weak).

While the phenomenology and basic physics of electronic transport in mesoscopic size systems are becoming well understood, it remains important to develop and improve effective stable methods for accurately and efficiently calculating the conductance in two- and three-dimensional systems that can treat arbitrary geometry, magnetic fields and potential drops across the device (to obtain the non-linear conductance), even at low temperatures where phonon scattering is not crucial. Other methods, such as the tight-binding method [14] and the finite-element method [15], have not been applied simultaneously to treat arbitrary geometry, magnetic fields and potential drops across the device, particularly when closed channels are important to converge the scattering calculation. Here we present a method that can treat all these issues and we explain the results of calculations using this method in simple physical terms. We find that the non-linear conductance as a function of the potential drop across heterostructure devices is shifted by applying a transverse magnetic field. The resonance voltage (i.e. the voltage such that $\mathrm{d}I/\mathrm{d}V = 0$) can therefore be modified by varying the magnetic field strength. We find resonances in the conductance as functions of potential drop and orifice width for wide orifice structures (when the width of the orifice is larger than that of the lead) due to the occurrence of closed orbits in the orifice. No resonance features appear in the non-linear conductance of crimped orifices as a function of potential drop; the conductance steadily increases with increased potential drop.

Consider the quantum-mechanical scattering at zero (or sufficiently small) temperature of a charged particle (electron or hole) of mass μ propagating across a heterojunction quantum well structure with potential drop ΔV across it, as shown in figure 1. The potential energy (i.e. for electron conduction, the bottom of the conduction band) with a potential drop ΔV across the device is shown versus position in the quantum well heterostructure, for a heterostructure composed of a semiconductor 2, semiconductor 1, semiconductor 2, semiconductor 1 and semiconductor 2 (figure 2). The system may be two dimensional, as represented in figure 2, or three dimensional with a non-negligible depth compared with the other dimensions. Figure 2 shows the case when the width $w(r)$ of the two-dimensional

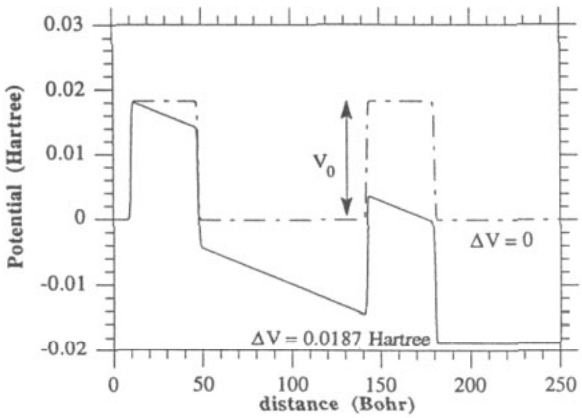

Figure 1. Quantum well potential: — · —, zero potential drop across the structure; ——, potential drop $\Delta V = 0.0187$ Hartree ($\simeq$ 0.5 eV). The barriers are somewhat rounded (see equation (28) for the form of the barriers).

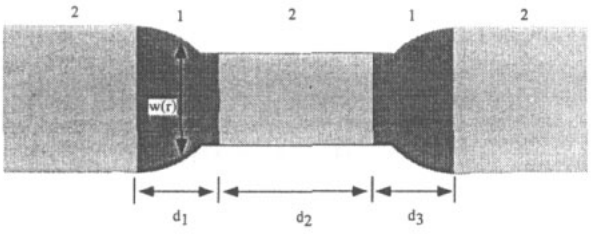

Figure 2. Two-dimensional pictorial representation of the quantum well heterostructure composed of two semiconductor materials sandwiched between each other. Depicted here is the case when the width $w(r)$ of the two-dimensional structure depends on the coordinate r along the current flow.

structure depends on the coordinate r along the current flow although the width may be constant, independent of r.

The conductance at zero temperature involves scattering that occurs at the Fermi energy (or an arbitrary temperature, see discussion related to equation (24)). Denoting the Fermi energy as $E_F = \hbar^2 k_F^2/2\mu$, the number of open channels on the left of the device is given for hard-wall boundary conditions by the integer $N_L = [k_F w/\pi]$ where the square brackets indicate the integer part of the argument. For example, if $1 < k_F w/\pi < 2$, only one channel is open on the left, and the asymptotic relative kinetic energy along the direction of current flow in this channel is given by $E = E_F - \hbar^2\pi^2/2\mu w^2$. The conductance at zero temperature is determined by the quantum-mechanical transmission probability from the left to the right of the system and therefore depends on the number of open channels and the transmission probability from right to left in each of these open channels. The number of open channels on the right depends on the potential drop ΔV across the device and is given by $N_R = [(2\mu(E + \Delta V))^{1/2} w/\pi\hbar]$ which need not equal N_L and, with sufficiently large ΔV, $N_R > N_L$. Our method can be easily applied to non-hard-wall boundary conditions (i.e. finite 'work function' potentials).

In the next section we describe the quantum scattering method used to determine the reflection and transmission scattering amplitude matrices and, from them, the conductance of the device. In section 3 we present the results of numerical calculations for the conductance and magnetoconductance of heterojunction quantum well structures and quantum dots. A summary and conclusion are presented in section 4.

2. Quantum scattering approach

We want to extract scattering information from the wavefunction $\Psi_{E,\gamma}$ for incident channel γ, for the Schrödinger equation at energy E:

$$H\Psi_{E,\gamma} = E\Psi_{E,\gamma}. \tag{1}$$

The wavefunction $\Psi_{E,\gamma}$ depends on the coordinate r for the motion along the current flow, and a set of 'internal' coordinates η that are orthogonal to r and can be expanded in terms of an adiabatic orthonormal internal state basis set $\{\psi_\gamma(\eta, r)\}$ that depends on the scattering coordinate r:

$$\Psi_{E,\gamma}(\eta, r) = \sum_{\gamma'} \psi_{\gamma'}(\eta, r)\frac{F_{\gamma',\gamma}(r)}{r}. \tag{2}$$

The sum here is over the number of channels (opened and closed) carried in the calculation. For simplicity, we take the boundary condition that the internal wavefunction vanishes at the edges of the device, $\eta = -w/2$, and $w/2$ (the case when the electronic wavefunction is taken to decay exponentially into the regions $\eta < -w/2$ and $\eta > w/2$ can be treated with not much more effort if the work functions of the materials are given). Let us consider three examples. Case (a) is where the width w is independent of r; $-w/2 \leqslant \eta \leqslant w/2$, $-\infty \leqslant r \leqslant \infty$ and $\psi_\gamma(\eta, r) = \sqrt{2/w}\sin[\gamma\pi(\eta + w/2)/w]$, where $\gamma = 1, 2, \ldots$. In this case the basis set of states $\{\psi_\gamma(\eta)\}$ is independent of r. Case (b) corresponds to case (a) in the presence of a finite perpendicular magnetic field. Here the Hamiltonian will contain first- and second-derivative coupling terms due to the presence of the magnetic field as described below. The Hamiltonian matrix is complex but Hermetian. Case (c) is the case in figure 2 with or without a magnetic field; the width w now depends on r and therefore the functions $\{\psi_\gamma(\eta, r)\}$ depend parametrically on r. Here the Hamiltonian will contain first- and second-derivative coupling terms due to the dependence of the internal basis set on r. If no magnetic field is present, the Hamiltonian matrix is real symmetric, and with a magnetic field it is complex Hermetian.

Calculation of the conductance in the presence of a magnetic field in *all* space requires the use of basis states that are eigenstates of the Hamiltonian with the magnetic field incorporated [16]. Such an approach is possible within the context of the invariant embedding procedure that we employ, but we do not do so here. Instead we take a different approach and let the magnetic field turn off as $r \to -\infty$ and $r \to \infty$. If the turn-off is sufficiently slow, scattering off the region where the magnetic field varies will be negligible and the adiabatic theorem ensures that asymptotic eigenstates develop adiabatically into the magnetic field states. The turn-off of the magnetic field is determined in terms of the parameter σ_H which characterizes the width of the region over which the magnetic field is turned off.

Matrix elements of the Hamiltonian between basis states (in atomic units) take the form

$$H_{\gamma\gamma'}(r) = \langle\psi_\gamma(\eta, r)|H|\psi_{\gamma'}(\eta, r)\rangle_\eta = \delta_{\gamma,\gamma'}\frac{p_r^2}{2\mu} - \frac{\mathrm{i}}{\mu}A_{\gamma,\gamma'}(r)p_r - \frac{1}{2\mu}B_{\gamma\gamma'}(r) + U_{\gamma,\gamma'}(r) \tag{3}$$

where the first-derivative coupling matrix $A_{\gamma,\gamma'}(r)$ and the second-derivative coupling matrix $B_{\gamma\gamma'}(r)$ vanish asymptotically as $r \to -\infty$ and $r \to \infty$. For case (a), $\mathbf{A} = \mathbf{B} = \mathbf{0}$. For case (b) with a magnetic field in the z direction of the form (one can replace r with x and η with y in equations (4) and (5) if this notation might be more familiar to the reader), $\mathbf{H} = H_0 q(r)\hat{\mathbf{k}}$, where $\hat{\mathbf{k}}$ is the unit vector in the direction of the magnetic field which is normal to the two-dimensional electron gas with $q(r)$ given by

$$q(r) = \begin{cases} \exp[-(r - r_1)^2/2\sigma_H^2] \\ 1 \\ \exp[-(r - r_2)^2/2\sigma_H^2] \end{cases} \quad \text{for} \quad \begin{cases} r \leqslant r_1 \\ r_1 \leqslant r \leqslant r_2 \\ r_2 \leqslant r \end{cases} \tag{4}$$

and σ_H is the width of the region in which the magnetic field is turned on. Choosing an electromagnetic gauge wherein the vector potential takes the form $H_0\eta q(r)\hat{\mathbf{i}}$, the Hamiltonian is given by

$$H = \frac{[p_r - H_0\eta q(r)/c]^2 + p_\eta^2}{2\mu} + V(r). \tag{5}$$

Hence, we obtain the following expressions for **A**, **B** and **U** in equation (3):

$$A_{\gamma,\gamma'}(r) = -\frac{\mathrm{i}q(r)}{\ell^2}Y_{\gamma,\gamma'} \tag{6}$$

$$B_{\gamma,\gamma'}(r) = -\frac{\mathrm{i}\mathrm{d}q(r)/\mathrm{d}r}{\ell^2}Y_{\gamma,\gamma'} - \frac{q(r)^2}{\ell^4}Y^2_{\gamma,\gamma'} \tag{7}$$

$$U_{\gamma,\gamma'}(r) = \left(V(r) + \frac{\gamma^2\pi^2}{2\mu w^2}\right)\delta_{\gamma,\gamma'} \tag{8}$$

where we used the definitions

$$\begin{aligned} Y_{\gamma,\gamma'} &= \frac{2}{w}\int_{-w/2}^{w/2}\mathrm{d}\eta \sin\left(\frac{\gamma\pi(\eta + w/2)}{w}\right)\eta \sin\left(\frac{\gamma'\pi(\eta + w/2)}{w}\right) \\ Y^2_{\gamma,\gamma'} &= \frac{2}{w}\int_{-w/2}^{w/2}\mathrm{d}\eta \sin\left(\frac{\gamma\pi(\eta + w/2)}{w}\right)\eta^2 \sin\left(\frac{\gamma'\pi(\eta + w/2)}{w}\right) \end{aligned} \tag{9}$$

and defined the magnetic length $\ell = (c/H_0)^{1/2}$ (in atomic units, $\ell = (\hbar c/eH_0)^{1/2}$ in Gaussian units). For case (c), the adiabatic basis state case with geometry in figure 2 and without magnetic field,

$$\begin{aligned} A_{\gamma,\gamma'}(r) &= \langle\psi_\gamma(\eta, r)|\frac{\partial}{\partial r}|\psi_{\gamma'}(\eta, r)\rangle_\eta \\ B_{\gamma\gamma'}(r) &= \langle\psi_\gamma(\eta, r)|\frac{\partial^2}{\partial r^2}|\psi_{\gamma'}(\eta, r)\rangle_\eta - \frac{\gamma^2\pi^2}{w^2}\delta_{\gamma,\gamma'}. \end{aligned} \tag{10}$$

Moreover, in the case with a magnetic field present on the structure shown in figure 2, we have

$$A_{\gamma,\gamma'}(r) = -\frac{\mathrm{i}q(r)}{\ell^2}Y_{\gamma,\gamma'} + \langle\psi_\gamma(\eta, r)|\frac{\partial}{\partial r}|\psi_{\gamma'}(\eta, r)\rangle_\eta \tag{6'}$$

$$\begin{aligned} B_{\gamma,\gamma'}(r) = &-\frac{\mathrm{i}\mathrm{d}q(r)/\mathrm{d}r}{\ell^2}Y_{\gamma,\gamma'} - \frac{q(r)^2}{\ell^4}Y^2_{\gamma,\gamma'} - \frac{2\mathrm{i}q(r)}{\ell^2}\langle\psi_\gamma(\eta, r)|\eta\frac{\partial}{\partial r}|\psi_{\gamma'}(\eta, r)\rangle_\eta \\ &+ \langle\psi_\gamma(\eta, r)|\frac{\partial^2}{\partial r^2}|\psi_{\gamma'}(\eta, r)\rangle_\eta \end{aligned} \tag{7'}$$

$$U_{\gamma,\gamma'}(r) = \left(V(r) + \frac{\gamma^2\pi^2}{2\mu w^2}\right)\delta_{\gamma,\gamma'}. \tag{8'}$$

In any case, the Hamiltonian involves the diagonal potential $\mathbf{U}(r)$, shown in figure 1, where $\mathbf{U}(r)$ has asymptotic properties $\mathbf{U}(+\infty) = -\Delta V\mathbf{1}$ (ΔV is the charge of the electron

times the voltage across the device) and $\mathbf{U}(-\infty) = \mathbf{0}$. It is important to note that the asymptotic nature of the potential $\mathbf{U}(r)$ is different as $r \to -\infty$ and $r \to \infty$. This is the reason that a scattering formulation appropriate for rearrangement collisions is necessary. The Schrödinger equation for the regular radial wavefunctions $F_{\gamma',\gamma}(r)$ is given by

$$\frac{\mathrm{d}^2}{\mathrm{d}r^2}\mathbf{F}(r) + \left(2\mu[E\mathbf{1} - \mathbf{U}(r)] + \mathbf{B}(r) + 2\mathbf{A}(r)\frac{\mathrm{d}}{\mathrm{d}r}\right)\mathbf{F}(r) = 0. \tag{11}$$

The asymptotic behaviour of the wavefunction $\mathbf{F}$ depends on whether the incident wave enters from the left or from the right.

In order to apply the invariant embedding method [11, 12], we cut the potential at $r = x_0$, and define a reference potential $\mathbf{V}(r)$ to be

$$\mathbf{V}(r) = \begin{cases} \mathbf{U}(-\infty) \\ \mathbf{U}(\infty) \end{cases} \qquad \text{for} \begin{cases} r \leqslant x_0 \\ r > x_0. \end{cases} \tag{12}$$

The remaining interaction potential $\mathbf{I}(r)$ is defined by

$$\mathbf{U}(r) - \frac{1}{2\mu}\mathbf{B}(r) = \mathbf{V}(r) + \mathbf{I}(r) \tag{13}$$

such that $\mathbf{I}(-\infty) = \mathbf{I}(\infty) = 0$. One now can define channel momenta on the left by

$$\mathbf{k}_l^2 = 2\mu[E\mathbf{1} - \mathbf{U}(-\infty)]$$

and on the right by

$$\mathbf{k}_r^2 = 2\mu[E\mathbf{1} - \mathbf{U}(\infty)].$$

The boundary conditions for the wavefunction for a wave incident from the left are

$$\begin{aligned} \mathbf{F}(r) &= \mathbf{k}_l^{-1/2}[\exp(\mathrm{i}\mathbf{k}_l r)\mathbf{1} + \exp(-\mathrm{i}\mathbf{k}_l r)\mathbf{R}] \qquad \text{as } r \to -\infty \\ \mathbf{F}(r) &= \mathbf{k}_r^{-1/2}\exp(\mathrm{i}\mathbf{k}_r r)\mathbf{T} \qquad \text{as } r \to \infty \end{aligned} \tag{14}$$

Similarly for the wavefunction $\tilde{\Psi}_{E,\gamma}(\eta, r) = \sum_{\gamma'} \psi_{\gamma'}(\eta, r)\tilde{F}_{\gamma',\gamma}(r)/r$ describing a wave incident from the right,

$$\begin{aligned} \tilde{\mathbf{F}}(r) &= \mathbf{k}_l^{-1/2}\exp(-\mathrm{i}\mathbf{k}_l r)\tilde{\mathbf{T}} \qquad \text{as } r \to -\infty \\ \tilde{\mathbf{F}}(r) &= \mathbf{k}_r^{-1/2}[\exp(-\mathrm{i}\mathbf{k}_r r)\mathbf{1} + \exp(\mathrm{i}\mathbf{k}_r r)\tilde{\mathbf{R}}] \qquad \text{as } r \to \infty. \end{aligned} \tag{15}$$

$\mathbf{T}$ and $\mathbf{R}$ are the transmission and reflection amplitudes for an initial wave incident from the left, and $\tilde{\mathbf{T}}$ and $\tilde{\mathbf{R}}$ are the transmission and reflection amplitudes for an initial wave impinging on the sample from the right. A unitary on-shell $\mathbf{S}$-matrix can be written in terms of the quantities $\mathbf{T}$, $\mathbf{R}$, $\tilde{\mathbf{T}}$ and $\tilde{\mathbf{R}}$ [17]:

$$\mathbf{S} = \begin{bmatrix} \mathbf{T} & \tilde{\mathbf{R}} \\ \mathbf{R} & \tilde{\mathbf{T}} \end{bmatrix}. \tag{16}$$

Note that one-dimensional scattering involves a two-channel quantum problem (**S** is a 2×2 matrix). The zero-order wavefunctions (in this case solutions to $p_r^2/2\mu + V$) are related to the solution of the Schrödinger equation for the case where the potential is the reference potential $\mathbf{V}(r)$ and are given by

$$\begin{aligned}
&\mathbf{h}^+(r) = \mathbf{k}_l^{-1/2}[\exp(\mathrm{i}\mathbf{k}_l r) + \exp(-\mathrm{i}\mathbf{k}_l r)\mathbf{r}] \qquad \text{when } r \leqslant x_0 \\
&\mathbf{h}^+(r) = \mathbf{k}_l^{-1/2}\exp(\mathrm{i}\mathbf{k}_r r)\mathbf{t} \qquad \text{when } r \geqslant x_0
\end{aligned} \tag{17}$$

$$\begin{aligned}
&\mathbf{h}^-(r) = \mathbf{k}_r^{-1/2}\exp(-\mathrm{i}\mathbf{k}_l r)\tilde{\mathbf{t}} \qquad \text{when } r \leqslant x_0 \\
&\mathbf{h}^-(r) = \mathbf{k}_r^{-1/2}[\exp(-\mathrm{i}\mathbf{k}_r r) + \exp(\mathrm{i}\mathbf{k}_r r)\tilde{\mathbf{r}}] \qquad \text{when } r \geqslant x_0
\end{aligned} \tag{18}$$

where $\mathbf{r}$, $\mathbf{t}$, $\tilde{\mathbf{r}}$ and $\tilde{\mathbf{t}}$ are the reflection and transmission amplitudes from the step of the potential. The derivation of the invariant embedding equations has been presented elsewhere [12]. Here, for completeness, we reproduce the algorithm used to calculate the **S**-matrix. The following set of equations for the **S**-matrix elements is obtained. One first solves for the reflection and transmission coefficients $\mathbf{T}(x)$, $\mathbf{R}(x)$, $\tilde{\mathbf{T}}(x)$ and $\tilde{\mathbf{R}}(x)$ which obey the following set of differential equations [12]:

$$\begin{aligned}
\frac{\mathrm{d}\mathbf{T}}{\mathrm{d}x} &= (\mathbf{h}^- + \tilde{\mathbf{R}}\mathbf{h}^+)2\mu\mathbf{W}^{-1}(\mathbf{I}\mathbf{h}^+ - \mu^{-1}\mathbf{A}\mathbf{h}_x^+)\mathbf{T} \\
\frac{\mathrm{d}\mathbf{R}}{\mathrm{d}x} &= \tilde{\mathbf{T}}\mathbf{h}^+ 2\mu\mathbf{W}^{-1}(\mathbf{I}\mathbf{h}^+ - \mu^{-1}\mathbf{A}\mathbf{h}_x^+)\mathbf{T} \\
\frac{\mathrm{d}\tilde{\mathbf{R}}}{\mathrm{d}x} &= (\mathbf{h}^- + \tilde{\mathbf{R}}\mathbf{h}^+)2\mu\mathbf{W}^{-1}[\mathbf{I}(\mathbf{h}^- + \mathbf{h}^+\tilde{\mathbf{R}}) - \mu^{-1}\mathbf{A}(\mathbf{h}_x^- + \mathbf{h}_x^+\tilde{\mathbf{R}})] \\
\frac{\mathrm{d}\tilde{\mathbf{T}}}{\mathrm{d}x} &= \tilde{\mathbf{T}}\mathbf{h}^+ 2\mu\mathbf{W}^{-1}[\mathbf{I}(\mathbf{h}^- + \mathbf{h}^+\tilde{\mathbf{R}}) - \mu^{-1}\mathbf{A}(\mathbf{h}_x^- + \mathbf{h}_x^+\tilde{\mathbf{R}})].
\end{aligned} \tag{19}$$

Here x is the cut-off of the potential, and as $x \to \infty$ the solution to the full potential is obtained [12]. Equation (19) gives the propagation equations for the **S**-matrix as a function of the cut-off. The initial conditions are chosen so that the **S**-matrix is unitary initially and equal to the unit matrix; hence $\mathbf{T}(-\infty) = \tilde{\mathbf{T}}(-\infty) = \mathbf{1}$, $\mathbf{R}(-\infty) = \tilde{\mathbf{R}}(-\infty) = \mathbf{0}$. The algorithm is based on evaluating the **S**-matrix as a function of the cut-off x from $x = 0$ until $x = x_0$ and so one should use the wavefunctions $\mathbf{h}^+(r)$ and $\mathbf{h}^-(r)$ given in equations (17) and (18) for $r \leqslant x_0$ only. The *full* **T**-, **R**-, $\tilde{\mathbf{T}}$- and $\tilde{\mathbf{R}}$-matrices are obtained when one takes into account the transmission and reflection from the step at x_0 to get

$$\mathbf{T} = \mathbf{t}\mathbf{T}(x_0) \qquad \mathbf{R} = \mathbf{r} + \tilde{\mathbf{t}}\mathbf{R}(x_0) \qquad \tilde{\mathbf{T}} = \tilde{\mathbf{t}}\tilde{\mathbf{T}}(x_0) \qquad \tilde{\mathbf{R}} = \tilde{\mathbf{r}} + \tilde{\mathbf{t}}\tilde{\mathbf{R}}(x_0). \tag{20}$$

The matrices $\mathbf{t}$, $\mathbf{r}$, $\tilde{\mathbf{t}}$ and $\tilde{\mathbf{r}}$ are determined by requiring that the zero-order wavefunctions $\mathbf{h}^+$ and $\mathbf{h}^-$ and their derivatives will be continuous at the matching point x_0. The resulting diagonal matrices $\mathbf{t}$, $\mathbf{r}$, $\tilde{\mathbf{t}}$ and $\tilde{\mathbf{r}}$ are given by

$$\begin{aligned}
t_{jj}(x_0) &= \frac{\sqrt{k_{lj} - k_{rj}}}{k_{lj} + k_{rj}}\exp[\mathrm{i}(k_{lj} - k_{rj})x_0] \\
r_{jj}(x_0) &= \frac{k_{lj} - k_{rj}}{k_{lj} + k_{rj}}\exp(2\mathrm{i}k_{lj}x_0)
\end{aligned} \tag{21}$$

$$\tilde{t}_{jj}(x_0) = \frac{\sqrt{k_{lj} - k_{rj}}}{k_{lj} + k_{rj}} \exp[\mathrm{i}(k_{lj} - k_{rj})x_0]$$
$$\tilde{r}_{jj}(x_0) = \frac{k_{rj} - k_{lj}}{k_{lj} + k_{rj}} \exp(-2\mathrm{i}k_{rj}x_0). \tag{22}$$

At zero temperature, the conductance is given by the expression [18]

$$g = (2e^2/h)\,\mathrm{Tr}(\mathbf{T}\mathbf{T}^\dagger) \tag{23}$$

where $\mathbf{T}$ is the transmission amplitude from left to right at the Fermi energy. At finite temperatures, the elastic scattering component of the conductance involves an average over the range of electron energies within the potential drop where the average takes the form

$$g = \frac{2e^2}{h}\Delta V^{-1}\int_0^\infty \mathrm{d}E\,\mathrm{Tr}[\mathbf{T}(E)\mathbf{T}^\dagger(E)][f(E - E_\mathrm{F}T) - f(E - E_\mathrm{F} - \Delta V, T)] \tag{24}$$

with $f(E, T)$ being the Fermi function $f(E, T) = [\exp(E/k_\mathrm{B}T) + 1]^{-1}$. In general, when a magnetic field is present, this expression needs to be modified to read

$$g = \frac{2e^2}{h}\Delta V^{-1}\int_0^\infty \mathrm{d}E\,\{\mathrm{Tr}[\mathbf{T}(E)\mathbf{T}^\dagger(E)]f(E - E_\mathrm{F}, T) - \mathrm{Tr}[\tilde{\mathbf{T}}(E)\tilde{\mathbf{T}}^\dagger(E)]f(E - E_\mathrm{F} - \Delta V, T)\} \tag{24'}$$

since $\tilde{T}_{n,m} \neq T_{m,n}$ but, for our geometry with symmetry around $\eta = 0$ (see equation (27)), $\mathrm{Tr}[\tilde{\mathbf{T}}(E)\tilde{\mathbf{T}}^\dagger(E)] = \mathrm{Tr}[\mathbf{T}(E)\mathbf{T}^\dagger(E)]$; so equation (24) is still valid. However, at finite temperatures, inelastic scattering effects due to the interaction of electrons with the phonon degrees of freedom play a significant role in determining the conductance. Our present formulation does not include the effects of the interaction with the phonon bath degrees of freedom.

The general relationships satisfied by the $\mathbf{S}$-matrix elements (defined in equation (16)) are, firstly, unitarity given by

$$\mathbf{S}(H)^\dagger\mathbf{S}(H) = \mathbf{S}(H)\mathbf{S}(H)^\dagger = \mathbf{1} \tag{25}$$

i.e.

$$\begin{bmatrix} \mathbf{T}^\dagger & \mathbf{R}^\dagger \\ \tilde{\mathbf{R}}^\dagger & \tilde{\mathbf{T}}^\dagger \end{bmatrix}\begin{bmatrix} \mathbf{T} & \tilde{\mathbf{R}} \\ \mathbf{R} & \tilde{\mathbf{T}} \end{bmatrix} = \begin{bmatrix} \mathbf{1} & \mathbf{0} \\ \mathbf{0} & \mathbf{1} \end{bmatrix} \qquad \begin{bmatrix} \mathbf{T} & \tilde{\mathbf{R}} \\ \mathbf{R} & \tilde{\mathbf{T}} \end{bmatrix}\begin{bmatrix} \mathbf{T}^\dagger & \mathbf{R}^\dagger \\ \tilde{\mathbf{R}}^\dagger & \tilde{\mathbf{T}}^\dagger \end{bmatrix} = \begin{bmatrix} \mathbf{1} & \mathbf{0} \\ \mathbf{0} & \mathbf{1} \end{bmatrix}$$

and, secondly, time reversal invariance given by

$$T_{m,n}(H) = \tilde{T}_{n,m}(-H)$$
$$R_{m,n}(H) = R_{n,m}(-H) \qquad \tilde{R}_{m,n}(H) = \tilde{R}_{n,m}(-H). \tag{26}$$

Moreover, in this specific case, $\mathbf{S}(H) = \mathbf{S}(-H)$ because of the reflection symmetry around $\eta(= y) = 0$, and hence

$$T_{m,n}(H) = \tilde{T}_{n,m}(H)$$
$$R_{m,n}(H) = R_{n,m}(H) \qquad \tilde{R}_{m,n}(H) = \tilde{R}_{n,m}(H). \tag{27}$$

3. Numerical examples

We present the results of calculations of the quantum scattering and the conductance and magnetoconductance of a quantum well structure of the type depicted in figure 1. We take the barriers to be somewhat 'rounded' so that a discontinuity does not occur in the potential (in any case, in reality, charge pile-up will 'round' the potential). The potential drop across the device is denoted as ΔV. The form of the potential that we use is given by

$$V(r) = \frac{V_0}{2}\left[\tanh\left(\frac{r-r_a}{\sigma_V}\right) - \tanh\left(\frac{r-r_a-d_1}{\sigma_V}\right)\right] + \frac{V_0}{2}\left[\tanh\left(\frac{r-r_a-d_1-d_2}{\sigma_V}\right) - \tanh\left(\frac{r-r_a-d_1-d_2-d_3}{\sigma_V}\right)\right] + \frac{\Delta V}{d_1+d_2+d_3}[(r-r_a)\theta(r-r_a)\theta(r_a+d_1+d_2+d_3-r) + (d_1+d_2+d_3)\theta(r-r_a+d_1+d_2+d_3)] \tag{28}$$

(here $\theta(r)$ is the usual step function) where the potential parameters are listed in table 1. The magnetic field is given by the form $\mathbf{H} = H_0 q(r)\hat{\mathbf{k}}$, with $q(r)$ specified in equation (4), with $x_1 = r_a + d_1$, and $x_2 = r_a + d_1 + d_2$. In practice, the magnetic field may be present within a large fraction of the leads as well. Here, however, we limit the magnetic field to be non-vanishing only within the heterostructure device. The present formalism can be extended to include a strong magnetic field acting on the entire system if the asymptotic states in the leads are properly chosen. For a weak magnetic field and for a sufficiently smooth interpolating function $q(r)$, the magnetic scattering is insignificant.

Table 1. Parameters used in the calculations.

Parameter	Value
μ	$0.1m_e$
V_0	0.018 38 Hartree (0.5 eV)
r_a	10 Bohr
$d_1 = d_3$	37.79 Bohr (20 Å)
d_2	94.48 Bohr (50 Å)
σ_H	1 Bohr
w_0	47.79 Bohr (25 Å)
σ_V	0.5 Bohr
σ_w	10 Bohr

Figure 3 shows the results of calculations of the transmission probability $|T_{1,1}|^2$ versus the potential drop across the device for a Fermi energy $E_F = 0.0234$ Hartree (1 Hartree = 27.21 eV is the atomic unit of energy) at which only one channel is open on the left (for a potential drop $\Delta V < 0.063$ Hartree at this Fermi energy, only one channel is open on the right). Note that the transmission probability $|T_{1,1}|^2$ equals the conductance g in units of $2e^2/h$, for this Fermi energy since there is only one channel open on both sides of the device. This Fermi energy corresponds to a relative kinetic energy on the left equal to a tenth of the barrier height, i.e. $V_0/10$. The conductance for three magnetic fields corresponding to inverse magnetic lengths $\ell^{-1} = 0$, 0.0398 and 0.05 Bohr^{-1} (1 Bohr = 0.5292 Å is the atomic unit of distance) are plotted in figure 3. For zero magnetic field, there is a

sharp resonance in the conductance at a value of $\Delta V = 0.0023$ Hartree, and a much broader resonance at $\Delta V = 0.02$ Hartree. These resonances are the well known single-channel resonance structures used to interpret the negative-differential-resistance phenomena occurring in Esaki diode devices. At these voltages, the electrons resonantly tunnel through the device. For magnetic field strengths such that the magnetic length is significantly larger than the width of the device, the effect of the magnetic field on the conductance is minimal. A visible effect of the magnetic field on the conductance occurs only for $\ell < 100$ Bohr ($\ell^{-1} > 0.01$ Bohr^{-1}) because the magnetic length must be comparable with or smaller than the system size for the effect of the magnetic field to be significant on the dynamics. At small values of ΔV, the conductance decreases with increasing magnetic field as is clearly evident from figure 3 (ℓ^{-1} is proportional to $H_0^{1/2}$). The resonance of the conductance moves to larger values of ΔV with increasing H_0. Figure 4 shows the conductance as a function of ℓ^{-1} for $\Delta V = 0$, 0.006236, 0.01247 and 0.01871 Hartree. The general trend of decreased conductance with larger magnetic field strength is evident from the precipitous drops of the conductance with increasing field strength, but the dependence of conductance versus H_0 is non-monotonic, and resonance structures as a function of H_0 occur. We should mention that we checked the convergence of our calculations with the number of channels by including more closed channels in the calculation and verifying that the results remain unchanged. It is worth pointing out here that our system is not disordered, and hence there is no characteristic of weak localization nor any effect of the magnetic field on the weak localization, such as negative magnetoresistance. Hence, the magnetic field serves as an additional parameter and its role as a time reversal breaking term within the present formalism will be investigated elsewhere.

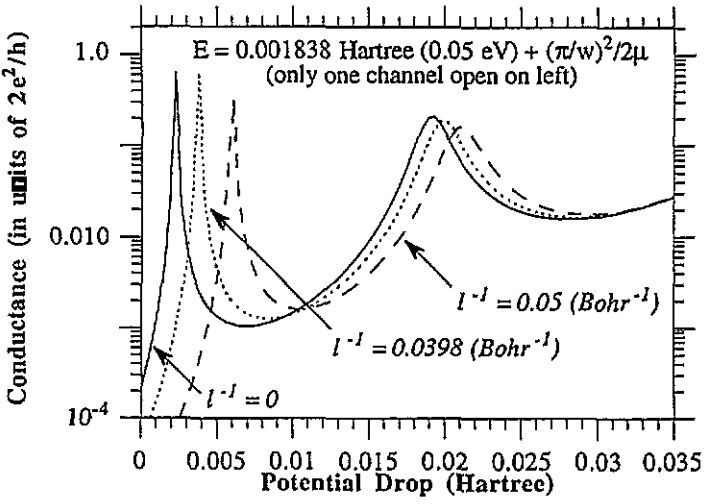

Figure 3. Conductance (in units of $2e^2/h$) versus the potential drop across the device for three magnetic fields corresponding to inverse magnetic lengths $\ell^{-1} = 0$, 0.0398 and 0.05 Bohr^{-1} for a Fermi energy $E_F = 0.0234$ Hartree at which only one channel is open on the left (and on the right for a potential drop $\Delta V < 0.063$ Hartree at this Fermi energy).

Let us now calculate the conductance at a somewhat higher Fermi energy, $E_F = 0.0886$ Hartree, where two channels are open. When $H_0 = 0$, the off-diagonal transmission

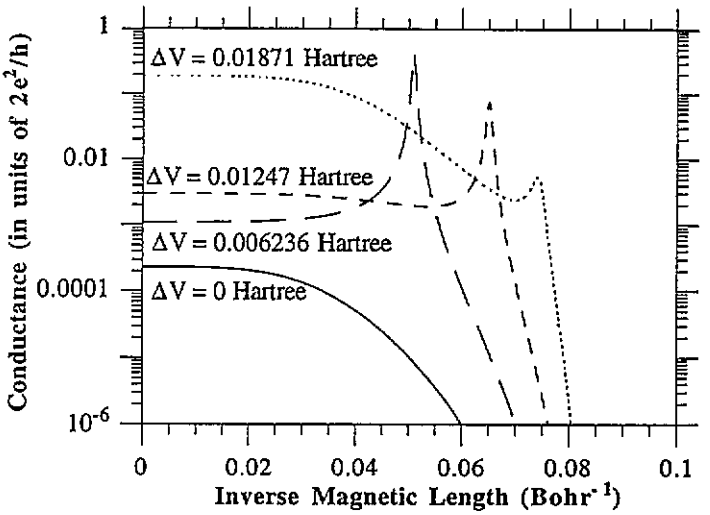

Figure 4. Conductance (in units of $2e^2/h$) versus inverse magnetic length ℓ^{-1} for four potential drops $\Delta V = 0$, 0.006 236, 0.012 47 and 0.018 71 Hartree, for Fermi energy $E_F = 0.0234$ Hartree.

and reflection amplitudes vanish, $|T_{i,i}|^2 + |R_{i,i}|^2 = 1$, $T_{i,i} = \tilde{T}_{i,i}$ and therefore $|R_{i,i}|^2 = |\tilde{R}_{i,i}|^2$. Figure 5 shows the transmission probabilities $|T_{1,1}|^2$ and $|T_{2,2}|^2$ versus potential drop for zero magnetic field, $\ell^{-1} = 0$. The transmission probability for the first (most open) channel is very close to unity for all potential drops but shows a very broad dip centred at around $\Delta V = 0.02$ Hartree. The probability $|T_{2,2}|^2$ shows resonance structures at around 0.0015 and 0.0185 Hartree. There is no coupling between the first and second channels when the magnetic field is zero. Figure 6 shows the transmission and reflection probabilities versus potential drop for a magnetic field corresponding to an inverse magnetic length $\ell^{-1} = 0.05$ Bohr^{-1}. It is interesting to note that a resonance structure occurs in all the transmission probabilities at $\Delta V = 0.011$ Hartree. At this value of potential drop, the off-diagonal transmission probabilities are about as large as the diagonal probabilities, i.e. $|T_{2,1}|^2 \simeq |T_{1,1}|^2$ and $|T_{1,2}|^2 \simeq |T_{2,2}|^2$. Moreover, the reflection probabilities also show resonances at this value of potential drop. Broader structure is evident at around $\Delta V = 0.0285$ Hartree. Once again, the structure is evident in all the transmission and reflection probabilities for flux emanating from the left of the system. We shall not pause to describe the transmission and reflections emanating from the right of the system, since these probabilities do not contribute to the conductance. Figure 7 shows the conductance $\mathrm{Tr}(\mathbf{T}\mathbf{T}^\dagger)$ versus ΔV for $\ell^{-1} = 0$, 0.0396 and 0.05 Bohr^{-1}. The conductance is roughly unity since the contributions $[\mathbf{T}\mathbf{T}^\dagger]_{1,1} = \sum_i |T_{i1}|^2$ and $[\mathbf{T}\mathbf{T}^\dagger]_{2,2} = \sum_i |T_{i2}|^2$ to the conductance are nearly unity and zero respectively. For $\ell^{-1} = 0$, the resonances at $\Delta V = 0.0015$ and 0.018 Hartree are due to the structure in $|T_{1,2}|^2$ and $|T_{2,2}|^2$ and, since there is no coupling of channels for $H_0 = 0$, in $|T_{2,2}|^2$ (see figure 6). For $\ell^{-1} = 0.05$ Bohr^{-1} (and $\ell^{-1} = 0.0396$ Bohr^{-1}), the structure near 0.011 Hartree (0.005 Hartree) is due to that in $[\mathbf{T}\mathbf{T}^\dagger]_{1,1}$.

We now turn to the case shown in figure 2 where the width of the device is a function of r. We take $w(r)$ to be of the form

$$w(r) = w_0 - \frac{\Delta w}{2}\left[\tanh\left(\frac{r - r_a - d_1}{\sigma_w}\right) - \tanh\left(\frac{r - r_a - d_1 - d_2 - d_3}{\sigma_w}\right)\right] \tag{29}$$

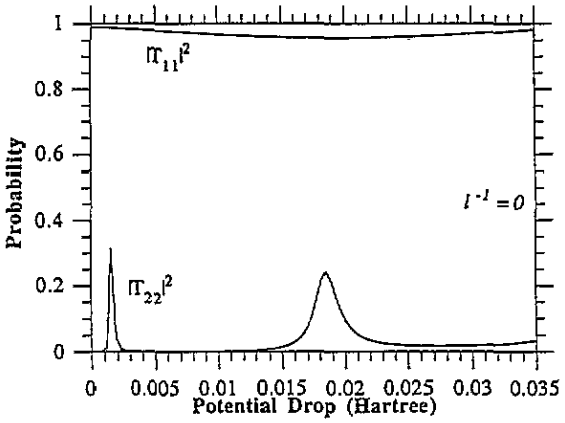

Figure 5. Transmission probabilities $|T_{1,1}|^2$ and $|T_{2,2}|^2$ versus potential drop for zero magnetic field for Fermi energy $E_F = 0.0886$ Hartree.

and choose w_0 and σ_w as listed in table 1, and $\Delta w = 10$ Bohr. We calculate the scattering amplitudes and the conductance versus both Δw and ΔV in the absence of a magnetic field. The following matrix elements are now required to proceed with the calculation:

$$\begin{aligned}\langle\psi_\gamma(\eta,r)|\frac{\partial}{\partial r}|\psi_{\gamma'}(\eta,r)\rangle_\eta &= \int_{-w/2}^{w/2}\mathrm{d}\eta\sqrt{\frac{2}{w}}\sin\left(\frac{\gamma\pi(\eta+w/2)}{w}\right)\frac{\partial}{\partial r}\left[\sqrt{\frac{2}{w}}\sin\left(\frac{\gamma'\pi(\eta+w/2)}{w}\right)\right]\\ &= \frac{-\pi\,\mathrm{d}w/\mathrm{d}r}{w^2}\frac{2\gamma'}{w}\int_{-w/2}^{w/2}\mathrm{d}\eta\sin\left(\frac{\gamma\pi(\eta+w/2)}{w}\right)\eta\cos\left(\frac{\gamma'\pi(\eta+w/2)}{w}\right)\\ &\quad -\frac{1}{2w}\frac{\mathrm{d}w}{\mathrm{d}r}\delta_{\gamma\gamma'}\end{aligned} \tag{30}$$

$$\begin{aligned}\langle\psi_\gamma(\eta,r)|\frac{\partial^2}{\partial r^2}|\psi_{\gamma'}(\eta,r)\rangle_\eta &= \frac{2}{w}\int_{-w/2}^{w/2}\mathrm{d}\eta\sqrt{\frac{2}{w}}\sin\left(\frac{\gamma\pi(\eta+w/2)}{w}\right)\frac{\partial^2}{\partial r^2}\left[\sqrt{\frac{2}{w}}\sin\left(\frac{\gamma'\pi(\eta+w/2)}{w}\right)\right]\\ &= -\left(\frac{\gamma'\pi\,\mathrm{d}w/\mathrm{d}r}{w^2}\right)^2 Y^2_{\gamma,\gamma'}+\frac{1}{2w^2}\left[\frac{3}{2}\left(\frac{\mathrm{d}w}{\mathrm{d}r}\right)^2-w\frac{\mathrm{d}^2w}{\mathrm{d}r^2}\right]\delta_{\gamma\gamma'}\\ &\quad +\frac{\pi}{w^3}\left[3\left(\frac{\mathrm{d}w}{\mathrm{d}r}\right)^2-w\frac{\mathrm{d}^2w}{\mathrm{d}r^2}\right]\frac{2\gamma'}{w}\\ &\quad \times\int_{-w/2}^{w/2}\mathrm{d}\eta\sin\left(\frac{\gamma\pi(\eta+w/2)}{w}\right)\eta\cos\left(\frac{\gamma'\pi(\eta+w/2)}{w}\right)\end{aligned} \tag{31}$$

and, if a magnetic field is present as well the additional matrix element,

$$\begin{aligned}\langle\psi_\gamma(\eta,r)|\eta\frac{\partial}{\partial r}|\psi_{\gamma'}(\eta,r)\rangle_\eta &= \int_{-w/2}^{w/2}\mathrm{d}\eta\sqrt{\frac{2}{w}}\sin\left(\frac{\gamma\pi(\eta+w/2)}{w}\right)\eta\frac{\partial}{\partial r}\left[\sqrt{\frac{2}{w}}\sin\left(\frac{\gamma'\pi(\eta+w/2)}{w}\right)\right]\end{aligned}$$

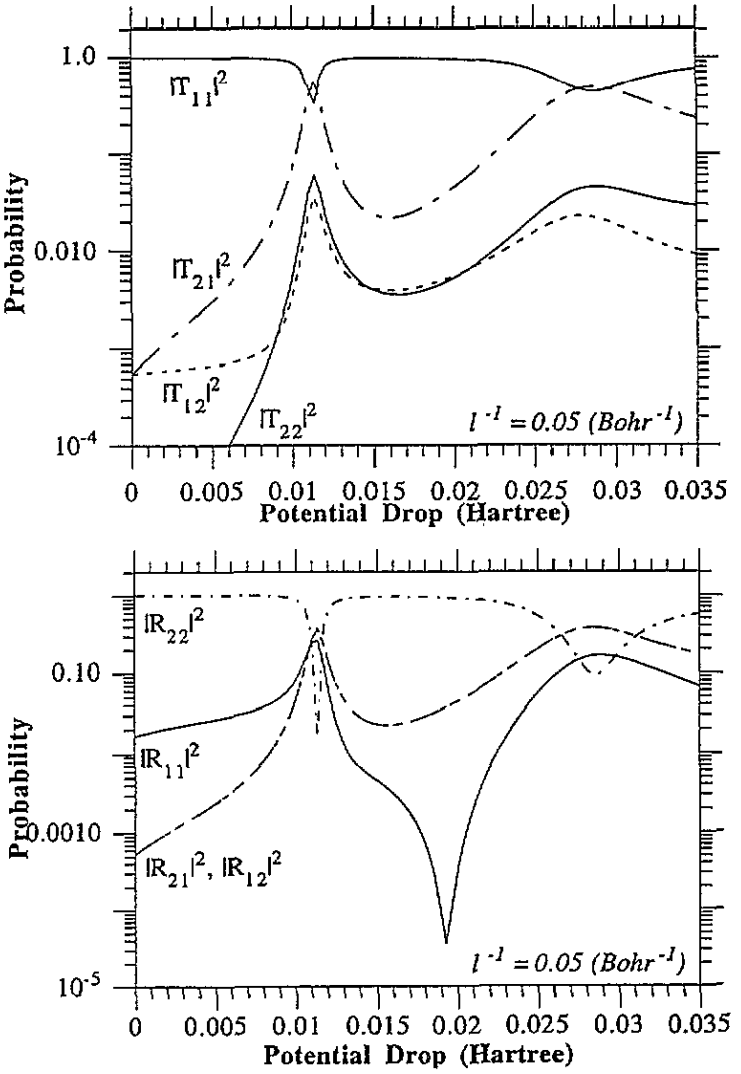

Figure 6. Transmission and reflection probabilities versus potential drop for a magnetic field corresponding to an inverse magnetic length $\ell^{-1} = 0.05$ Bohr^{-1} and Fermi energy $E_F = 0.0886$ Hartree.

$$= \frac{-\pi\, dw/dr}{w^2}\frac{2\gamma'}{w}\int_{-w/2}^{w/2} d\eta \sin\left(\frac{\gamma\pi(\eta + w/2)}{w}\right)\eta^2 \cos\left(\frac{\gamma'\pi(\eta + w/2)}{w}\right)$$

$$- \frac{1}{2w}\frac{dw}{dr}Y_{\gamma,\gamma'} \tag{32}$$

is also needed. All the integrals can be analytically performed, and the calculations are therefore of a similar nature to those performed where the width is not a function of r.

It is interesting to note that the second-derivative coupling matrix elements $\langle\psi_\gamma(\eta, r)|(\partial^2/\partial r^2)|\psi_{\gamma'}(\eta, r)\rangle_\eta$ (i.e. the B term; see equation (10)) can be calculated in terms of the first-derivative coupling matrix elements $\langle\psi_\gamma(\eta, r)|(\partial/\partial r)|\psi_{\gamma'}(\eta, r)\rangle_\eta$ (i.e. the

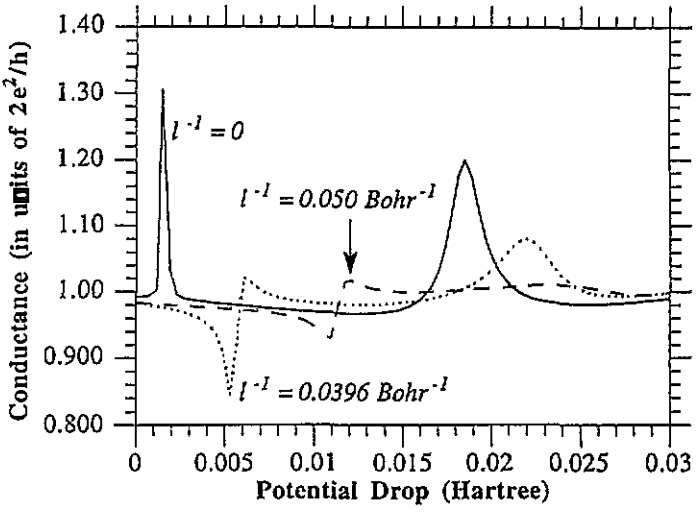

Figure 7. Conductance $\mathrm{Tr}[\mathbf{T}\mathbf{T}^{\dagger}]$ versus potential drop ΔV for inverse magnetic length $\ell^{-1} = 0$, 0.0396 and 0.05 Bohr^{-1}.

A term; see equation (10)) by using closure:

$$\langle\psi_\gamma(\eta,r)|\frac{\partial^2}{\partial r^2}|\psi_{\gamma'}(\eta,r)\rangle_\eta = \langle\psi_\gamma(\eta,r)|\frac{\partial}{\partial r}\sum_\alpha|\psi_\alpha(\eta,r)\rangle_\eta\langle\psi_\alpha(\eta,r)|\frac{\partial}{\partial r}|\psi_{\gamma'}(\eta,r)\rangle_\eta$$

$$= \sum_\alpha A_{\gamma,\alpha}(r)A_{\alpha,\gamma'}(r) + \frac{\mathrm{d}}{\mathrm{d}r}A_{\gamma,\gamma'}(r). \tag{33}$$

This is often used in transforming an adiabatic formulation to a diabatic formulation [19], a procedure that has been necessary in the past because adequate propagators for the Schrödinger equation with the first-derivative coupling term have not been available. However, a *complete* set of states is necessary to make this statement true. As an example of the problems that can arise in trying to use this closure relationship with a finite number of basis states, let us investigate the relationship (33) with only two channels:

$$\langle\psi_\gamma(\eta,r)|\frac{\partial^2}{\partial r^2}|\psi_{\gamma'}(\eta,r)\rangle_\eta \approx \langle\psi_\gamma(\eta,r)|\frac{\partial}{\partial r}\sum_{\alpha=1}^{2}|\psi_\alpha(\eta,r)\rangle_\eta\langle\psi_\alpha(\eta,r)|\frac{\partial}{\partial r}|\psi_{\gamma'}(\eta,r)\rangle_\eta$$

$$= \sum_{\alpha=1}^{2} A_{\gamma,\alpha}(r)A_{\alpha,\gamma'}(r) + \frac{\mathrm{d}}{\mathrm{d}r}A_{\gamma,\gamma'}(r). \tag{34}$$

For the two lowest-energy basis states, i.e. α, γ and γ' restricted to 1 and 2, we find using equation (30) that $A_{i,j}(r) = 0$ for $i, j = 1, 2$. Using equation (31), we find that the $\mathbf{B}(r) \neq 0$ for $i, j = 1, 2$ (the diagonal elements of $\mathbf{B}$ are non-vanishing). This exact result for $B_{i,j}(r)$ with $i, j = 1, 2$, is in contradiction to equation (34) ($A_{i,j}(r) = 0$ for $i, j = 1, 2$), but of course is not in contradiction to equation (33), since $A_{i,j}(r) \neq 0$ for all i, j. Thus it is clear that using the closure relationship, equation (33), but taking only a finite number of basis states in this relationship can yield incorrect results. This is a dazzling demonstration of the danger inherent in the standard procedure of transforming an adiabatic formulation within

a finite number of adiabatic basis states to a diabatic formulation with the same number of diabatic basis states [20].

Before presenting the conductance for the case of finite V_0, it is of interest to present the case when $V_0 = 0$, i.e. the case of an entirely flat potential. The only contributions to the potential are due to the r-dependent 'orifice', i.e. the r dependence of $w(r)$, and the linear potential drop across the device. A larger number of basis states need to be used in order for the calculations to converge with regard to the number of basis states in this case. We used eight channels for these calculations (of which only two are open on the right). Figure 8 shows the conductance versus Δw and ΔV. Let us first consider $\Delta V = 0$. When $\Delta w = 0$, two channels are open and the transmission in each channel is unity. Hence, $g = 2$. As Δw increases, the width of the orifice becomes narrower and the conductance decreases monotonically until only one mode remains open, and a plateau region with $g \simeq 1$ is encountered. At about $\Delta w = 24$ Bohr the conductance decreases rapidly to a region where $g \simeq 0$ for $\Delta w > 27$ Bohr. This is the well known phenomenon of quantized conductance [21]. For large negative Δw the conductance begins to oscillate as a function of Δw owing to the occurrence of closed orbits in the sample [22]. As ΔV begins to increase, there is a general trend of increased conductance in those regions of Δw where the conductance quantization changes for $\Delta V = 0$, i.e. near $\Delta w \approx 0$ and $\Delta w \simeq 27$. Moreover, resonance structures appear as indentations in the conductance in the region $\Delta w < -20$ and $\Delta V > 0$. We have not analysed the in-depth nature of these resonances but only note their presence.

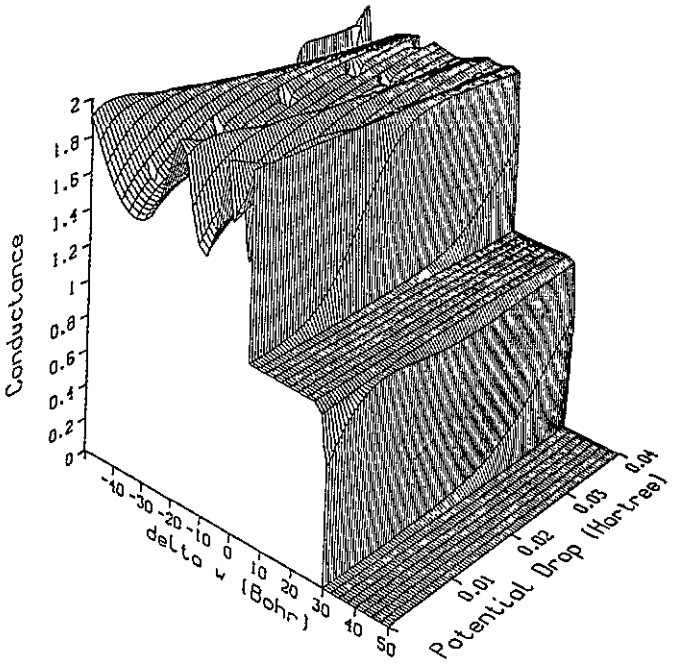

Figure 8. Conductance versus Δw and ΔV when $V_0 = 0$.

We now revert to the case of $V_0 = 0.5$ eV and present the results for the conductance versus Δw and ΔV in figure 9. The cut along $\Delta w = 0$ corresponds to the case shown in figure 3 (without a magnetic field). For $\Delta w > 27$ and small ΔV, there is a rapid drop in

the conductance because even the highest relative kinetic energy channel experiences severe problems penetrating the structure (recall that positive Δw means that the width decreases; see equation (29)). While there is some difference in the conductance for $\Delta w > 0$ in this case compared with the $V_0 = 0$ case in figure 8, the major differences are for $\Delta w \leqslant 0$. In this region a series of resonance structures affect the conductance as a function of Δw and ΔV. Experimentally, thermal averaging at finite temperatures (equation (24)) and phonon scattering effects will tend to smear the sharp resonance features obtained in the zero-temperature results.

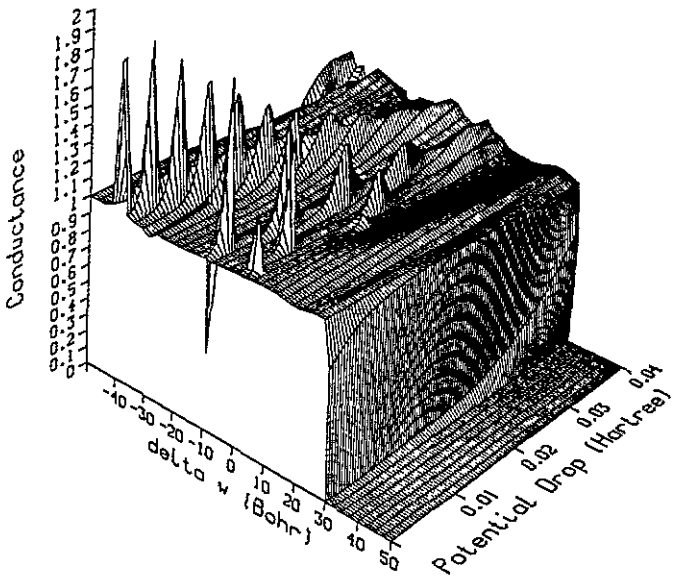

Figure 9. Conductance versus Δw and ΔV when $V_0 = 0.5$ eV.

4. Summary and conclusion

The invariant embedding method employed here is a stable and efficient technique for calculating the multichannel reflection and transmission amplitudes of quantum well structures, quantum dots and semiconductor or metallic microstructures and, from them, the low-temperature conductance and magnetoconductance of these structures (higher-temperature conductance can also be obtained but the effect of phonon scattering is not included in our present formulation). One-, two- and three-dimensional systems can be treated with this method, and the details of the geometry of the system can be easily included within the calculation because the method is capable of treating the scattering in an adiabatic basis set formulation. Our algorithm can accurately propagate across large (classically forbidden and open) regions. This method is well suited to carrying out calculations of the conductance and magnetoconductance of mesoscopic size structures where the three-dimensional geometrical structure of the device can be correctly incorporated into the calculation. Using our method, we find that the non-linear conductance as a function of the potential drop across the heterostructure device is shifted by applying a transverse magnetic field. Hence, the resonance voltage at which $dI/dV = 0$ can be modified by

varying the magnetic field strength. We find resonances in the conductance as a function of potential drop and orifice width for wide orifice structures (when the size of the lead is smaller than the size of the orifice) due to the occurrence of closed orbits in the orifice. No resonance features appear in the non-linear conductance of crimped orifices as a function of potential drop; the conductance steadily increases with increasing potential drop.

Application of the invariant embedding method to determine the conductance of devices with arbitrary geometry and arbitrary position of the leads requires using a coordinate system that is more involved than the coordinate system that we used here for describing motion along the current flow and perpendicular to it. No formulations along these lines have as yet been attempted. Moreover, modelling of four- and six-port conductance experiments requires a multi-arrangement scattering theory [23] for the multiple leads. This too has not yet been attempted within the context of the invariant embedding method.

Finally, we mention some additional physical phenomena which can be investigated using the present formalism. The first phenomenon is related to our calculations of the magnetoconductance for $\Delta w > 0$. If $\Delta w \gg w$, $V_0 = 0$ and $\Delta V = 0$ (the linear conductance regime), we may regard our two-(or three-)dimensional system as a large region with reflecting walls in which the motion of electrons is ballistic, attached to two narrow leads. An experimental study of the magnetoconductance of such structures has recently been reported [24]. It is expected that the transmission of the system is directly related to the spectrum of single-particle states in the region. In particular, if in this two-dimensional shape the motion of classical particles is chaotic (e.g. as in a stadium geometry), the spectrum of a quantum-mechanical system is determined by an ensemble of random matrices. In the absence of a time reversal breaking term in the Hamiltonian, the pertinent set of random matrices is the Gaussian orthogonal ensemble (GOE). On the other hand, in the presence of a time reversal breaking term in the Hamiltonian, the pertinent set of random matrices is the Gaussian unitary ensemble (GUE). Calculation of the conductance as a function of the magnetic field starting from zero magnetic field will then provide an interesting quantum physical scenario of passage from the GOE to GUE universality class in systems which are not random but are classically chaotic. It has been suggested [25] that in this case the conductance can be evaluated in a method similar to that used in the evaluation of **S**-matrix elements in compound nuclear reactions, employing supersymmetry techniques, and that the behaviour of the conductance as a function of the magnetic field is universal. Our formalism should allow numerical investigation of these ideas.

The second additional phenomenon for which the present formalism is suitable is determination of the current–voltage fluctuation characteristics in mesoscopic systems. In this case we have in mind a disordered system in the non-linear conductance regime. Let $g(\Delta V_1)$ and $g(\Delta V_2)$ be the conductances evaluated for two different potential drops, and consider the quantity

$$K(\Delta V_1, \Delta V_2) = \langle g(\Delta V_1) g(\Delta V_2) \rangle - \langle g(\Delta V_1) \rangle \langle g(\Delta V_2) \rangle \tag{35}$$

where $\langle O \rangle$ denotes the disorder-averaged observable O. This correlation function plays an important role in the physics of non-linear conductance in disordered systems. It has been studied and evaluated within the diffusion approximation by Larkin and Khmelnitskii [26], and some pertinent experiments for its measurement have been reported recently [27]. Our formalism allows the detailed numerical study of the fluctuations in the current–voltage characteristics of mesoscopic systems. A third phenomenon is the transition between vacuum tunnelling and contact between two pieces of metal [28]. In fact, given the very general nature of the scattering technique developed here, it is likely that many additional phenomena will be able to be studied using this formulation.

Acknowledgments

This research is funded in part by grants from the US–Israel Binational Science Foundation and the Israel Council of Higher Education.

References

[1] Tsu R and Esaki L 1973 *Appl. Phys. Lett.* **22** 562
Esaki L 1986 *IEEE J. Quantum Electron.* **QE-22** 1611; 1985 *Synthetic Modulated Structures* ed L L Chang and B C Giessen (Orlando, FL: Academic) pp 3–41
Esaki L and Tsu R 1969 *IBM J. Res. Note* **RC-2418**
Chang L L, Esaki L and Tsu R 1974 *Appl. Phys. Lett.* **24** 593
Esaki L and Chang L L 1974 *Phys. Rev. Lett.* **33** 495
[2] Dingle R 1975 *Festkörperprobleme (Advances in Solid State Physics)* vol XV (Braunschweig: Vieweg) p 21
Dingle R, Wiegmann W and Henry C H 1974 *Phys. Rev. Lett.* **33** 827
Dingle R, Stormer H L, Gossard A C and Wiegmann W 1978 *Appl. Phys. Lett.* **33** 665
[3] Chang L L and Ploog K (ed) 1985 *Molecular Beam Epitaxy and Heterostructures* (Dordrecht: Nijhoff)
Chang L L and Giessen B C (ed) 1985 *Synthetic Modulated Structures* (Orlando, FL: Academic)
Parker E H C (ed) 1985 *The Technology and Physics of Molecular Beam Epitaxy* (New York: Plenum)
[4] Thouless D J 1974 *Phys. Rep.* **13** 93; 1979 *Ill Condensed Matter* ed G Toulouse and R Balian (Amsterdam: North-Holland) p 1
[5] Altshuler B L, Aronov A G and Spivak B Z 1981 *JETP Lett.* **33** 94
[6] Ando T, Fowler A B and Stern F 1982 *Rev. Mod. Phys.* **54** 437
Lee P A and Ramakrishnan T V 1985 *Rev. Mod. Phys.* **57** 287
[7] Band Y B and Efrima S 1983 *Phys. Rev.* B **28** 4126
Band Y B and Avishai Y 1986 *Phys. Rev.* B **34** 3429
Avishai Y and Band Y B 1987 *Phys. Rev. Lett.* **58** 2251
[8] Kalaba R and Kagiwada D H 1974 *Integral Equations via Imbedding Methods* (Reading, MA: Addison-Wesley)
Scott R 1973 *Invariant Imbedding and Its Application to Ordinary Differential Equations* (Reading, MA: Addison-Wesley)
[9] Singer S J, Freed K F and Band Y B 1982 *J. Chem. Phys.* **77** 1942
[10] Singer S J, Lee S, Freed K F and Band Y B 1987 *J. Chem. Phys.* **87** 4762
[11] Tuvi I and Band Y B 1993 *J. Chem. Phys.* **99** 9697
Band Y B and Tuvi I 1993 *J. Chem. Phys.* **99** 9704
[12] Band Y B and Tuvi I 1994 *J. Chem. Phys.* **100** 8869–76
[13] Sze S M 1981 *Physics of Semiconductor Devices* 2nd edn (New York: Wiley) ch 9
Ando Y and Itoh T 1987 *J. Appl. Phys.* **61** 1497
Lui W W and Fukuma M 1986 *J. Appl. Phys.* **60** 1555
Datta S, Melloch M, Bandyopadhyay S, Noren R, Vaziri M, Miller M and Reifenberger R 1986 *Phys. Rev. Lett.* **55** 2344
Vinter B 1984 *Appl. Phys. Lett.* **44** 307
Smoliner J, Hauser M, Gornik E and Weimann G 1987 *Appl. Phys. Lett.* **52** 33
Vassell M O, Lee J and Lockwood H F 1980 *J. Appl. Phys.* **54** 5206
Cahay M, McLennan M, Datta S and Lundstrom M S 1987 *Appl. Phys. Lett.* **50** 612
Ohnishi H, Inata T, Muto S, Yokoyama N and Shibatomi A 1986 *Appl. Phys. Lett.* **49** 1248
[14] Lent C S and Kirkner D J 1990 *J. Appl. Phys.* **67** 6353
[15] Sols F, Macucci M, Ravaioli U and Hess K 1989 *J. Appl. Phys.* **66** 3892
[16] Avishai Y and Band Y B 1989 *Phys. Rev. Lett.* **62** 2527–30
Schulte R L, Wyld H W and Ravenhall D G 1990 *Phys. Rev.* B **41** 12 760
[17] Avishai Y and Band Y B 1985 *Phys. Rev.* B **32** 2674
[18] Fisher D S and Lee P A 1981 *Phys. Rev.* B **23** 6851
Lee P A and Fisher D S 1981 *Phys. Rev. Lett.* **47** 882
[19] van Dishoeck E F, van Hemert M C, Allison A C and Dalgarno A 1984 *J. Chem. Phys.* **81** 5709
[20] Band Y B and Tuvi I 1995 Convergence of diabatic to adiabatic scattering calculations *Phys. Rev.* A 51 R3403

[21] van Wees B J, van Houten H, Beenakker C W J, Williamson J G, Kouwenhoven L P, van der Marel D and Fuxton C T 1988 *Phys. Rev. Lett.* **60** 848
Wharam D A, Thornton T J, Newbury R, Pepper M, Ajmed H, Frost J E F, Hasko D G, Peacock D C, Ritchie D A and Jones G A C 1988 *J. Phys. C: Solid State Phys.* **21** L209
Avishai Y and Band Y B 1989 *Phys. Rev.* B **40** 12535
Szafer A and Stone A D 1989 *Phys. Rev. Lett.* **62** 300
[22] Avishai Y and Band Y B 1990 *Phys. Rev.* B **41** 3253
[23] Mrugala F 1993 *Int. Rev. Phys. Chem.* **12** 1
[24] Marcus C M, Rimberg A J, Westervelt R M, Hopkins P F and Gossard A C 1992 *Phys. Rev. Lett.* **69** 506
[25] Weidenmuller H A 1994 *Max Planck Institute Preprint*
[26] Larkin A I and Khmelnitskii D E 1986 *Sov. Phys.–JETP* **64** 1075
[27] Ralph D C, Ralls K S and Buhrman R A 1993 *Phys. Rev. Lett.* **70** 986
[28] Krans J M, Muller C J, Yanson I K, Govaert Th C M, Hesper R and van Ruitenbeek J M 1995 *Phys. Rev.* B at press